Full Paper

Propellants, Explosives, Pyrotechnics

DOI: 10.1002/prep.201800080

Compression and Shear Experimental Study of PBX Explosive

Peng Chen,[a] Baohui Yuan,*[a] Rong Chen,[b] and Kepeng Qu[a]

Abstract: Generate compress-shear loading on Polymer Bonded Explosive (PBX) specimens. The research was carried out to determine the pressure and macroscopic temperature variation occurring in the specimen by using a pressure sensor and a thermocouple. High-speed photography was used to reveal the macroscopic ignition phenomena. X-ray diffraction (XRD) was used to study the material composition of raw and recovered specimens. The results of the experiments described here clearly show that specimens underwent crush, melt and ignition from impact to reaction. At the same time, the relative content of aluminium decreased. Compared to the direct impact results from split Hopkinson compression-shear bar tests, the drop-weight loading pulse is longer, so PBX specimens ignite more easily.

Keywords: PBX · drop-weight experiment · compress and shear load · reaction threshold

1 Introduction

Polymer Bonded Explosives (PBX) are the most important energy destruction resource and are widely used in the powder charges of conventional weapons [1–4]. During transportation, storage and assembling of devices, PBX often undergo pressure and shear loading instead of simply compression or tension. This type of loading introduces friction which leads to the sensitiving of PBXS. In other words, the accumulation of frictional heating can lead to an accidental ignition, which is directly related to the safety of PBXS [5]. Drop-weight and split Hopkinson pressure bars have been used to study the ignition properties of PBX. Drop-weights are widely used as one of the standard tests for the impact sensitivity of explosives and are available in the strain rate range of $10 \sim 1000\ s^{-1}$ [3]. Typical experiments in the drop-weight impact test use several milligrams of explosive or propellant which are subjected to the drop if a several kilogram weight to observe whether the specimen reacts [6]. Although there have been many experiments in this area, the ignition mechanisms are not well understood. In most of the impact sensitivity tests, the drop-weight systems are merely used as a test method. So there is a need to study the ignition produced by the drop-weight.

Due to the complexity of ignition which is related to hot spot formation, reaction growth and transition to detonation, the foundation theory of ignition has been pursued [7]. McIntosh et al. [8] and Brindley et al. [9] have studied a mathematical model to describe ignition of a reactive material and presented reasonable explanations for the ignition and initial combustion waves phenomenon. In order to investigate the hot spot characteristics of energetic crystals, Armstrong et al. [10] discovered the dimensional scale which is the dominant factor for the mechanical forces and deformations of energetic materials. While Wu [11] and Collins et al [12] proposed a model for hot spot formation in shocked energetic materials, the model was used to evaluate where the hot spot form due to void collapse, and also showed the results of the effect on the sensitivity of the material. Besides the research of mesoscale hot spot model, Raftenberg et al. [13] used finite element simulation to study the impact deformation of energetic materials. Czerski et al. [14] studied the four-step HMX kinetic model with an impact induced friction ignition mechanism of PBX. This model can accurately predict the timing and temperature behavior of reaction and ignition. The four-step HMX kinetic model showed good agreement with the drop-weight impact experiments.

At the same time, many experiments on impact ignition have been widely interpreted using the theory of hot spot model. Balzer et al. [6] and Hunt et al. [15] used drop-weight experiments to study the sensitivity of different grain size explosives and determined the mechanisms by which ignition occurred in specimens. With the aid of high-speed cameras and heat sensitive film, they found the main reason for ignition. Gruau et al. [16] also used the classical Steven test to investigate the ignition of explosives under low velocity impact, visualizing the ignition location and the ignition time with the help of numerical simulation. A hy-

[a] *P. Chen, B. Yuan, K. Qu*
Xi'an Modern Chemistry Research Institute
Xi'an, Shannxi, 710065 (P. R. China)
**e-mail: ybhybh59@sina.com*
[b] *R. Chen*
National University of Defense Technology
Changsha, Hunan, 410073 (P. R. China)
Fax: (+86) 29–88291506

brid drop-weight-Hopkinson bar system was used to determine the ignition threshold of PBXS [17]. The threshold for ignition can be quantified in terms of several parameters.

In order to study the mechanics and ignition properties of PBXS under drop-weight impact loading, this paper proposes a novel method using pressure sensors and thermocouples to measure the macro pressure and temperature variation. The ignition phenomenon and flame temperature are recorded with the aid of high-speed and infrared cameras.

2 Experiment

2.1 Drop-Weight Apparatus

The impact loading system consists of a drop-weight compression-shear system, a high-speed camera and an FLIR infrared camera (Figure 1(a)). The Figure 1 (b) shows a partially enlarged detail of the compression-shear system. This system consists of a block of steel with mass 10 kg, that can be dropped from a height of up to 2.5 m guided by two rods. The falling drop-weight directly impacts the wedge-head, which then compresses and shears the specimens under the two wedge surfaces, which are perpendicular to each other. A thermocouple is placed under the left specimen and a pressure sensor is placed under the right specimen. These sensors are used to measure changes of temperature and pressure. In order to ensure the stability of the compression-shear system during the experiment, the wedge base was fixed to the test platform. The theoretical maximum impact velocity from the full drop height is 7 m/s. However, due to friction between the drop-weight and the guiding rods, the maximum velocity was 6.5 m/s (measured using digital image correlation technology).

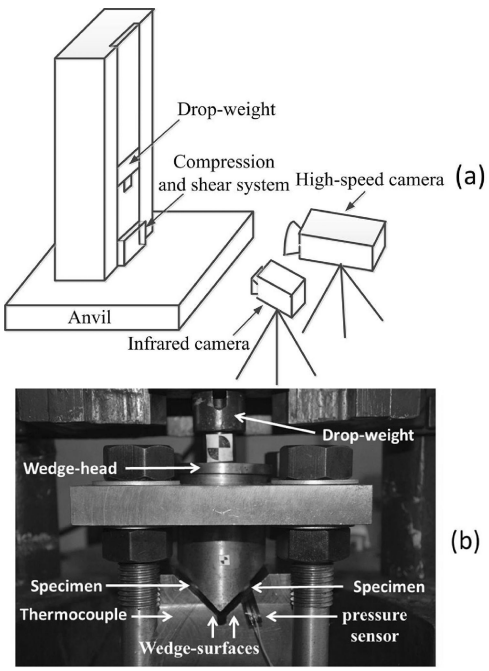

Figure 1. (a) Schematic drawing of drop-weight system,(b) Compression and shear system.

2.2 Specimen

RDX and Al powders were pressed into circular discs using a mould. Both powders used in this set of experiments were supplied in ultrafine and conventional grain size. The mass of the specimen shown in Figure 2 was 0.79 g, the thickness was 4 mm and the diameter was 12 mm.

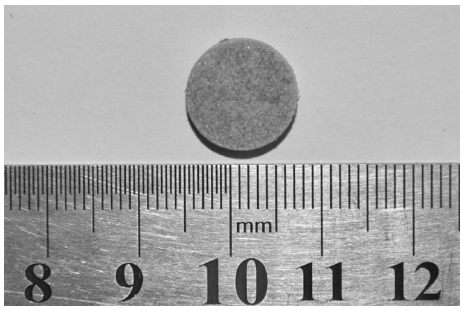

Figure 2. Specimen.

2.3 Calibration of Thermocouple

In order to obtain the temperature changes in the PBX explosive reaction, A13-E type thermocouples producted by the US Nanmac company was used. The diameter of the thermocouple was 0.1 mm. Because the thermocouple can generate thermoelectric power by itself at different temperatures, there is no need to supply external power. In the experiment, the thermoelectric output generated by the thermocouple was directly feed into a dynamic strain amplifier (100 ×), finally stored and displayed using a oscilloscope.

Before experiment, the thermocouples were calibrated. Firstly, two thermocouples were selected randomly, and compared with the readings of a thermometer both being placed in water. The output of a standard thermometer and the thermocouple voltage were recorded using an oscilloscope. The relationship between voltage and temperature is shown in Figure 3. As can be seen from the figure, the voltage increased linearly with temperature, according to the relation $\Delta = k\Delta V$, the values of k for the two thermocouples being 0.187 and 0.185 K/mV, then average was 0.186 K/mV.

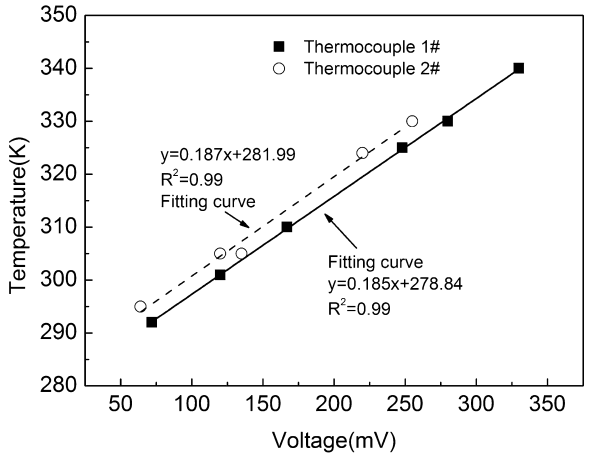

Figure 3. Calibration curves of thermocouples.

2.4 High-Speed Photography

In this experiment, images with a resolution of 768 × 640 pixels and a frame rate of 10000 fps (i.e, an inter-frame time of ~100 μs) were recorded with the help of a Photron FASTCAMSA-1 high-speed camera. The images were synchronised with the pressure-time curves.

3 Results and Discussion

3.1 Pressure of Specimen on the Loading and Wedge-Head Velocity Analysis

The specimens were symmetrically mounted between the wedge-head and wedge-surfaces, while the pressure sensor and thermocouple were placed beneath the specimen. Then the drop-weight was dropped from different heights to impact the wedge-head. Figure 4 shows a schematic of the specimen, the angle θ was 90°. As the loading continues, it induces a compressive stress F_p which is perpendicular to the surface and a shear stress F_s which is parallel to the surface. Then the relationship of F_p, F_s and F is:

$$\frac{F_p}{\sin\frac{\theta}{2}} + \frac{F_s}{\cos\frac{\theta}{2}} = F \tag{1}$$

Figure 5 shows the deformation of the specimen under the compression and shear load. When the wedge-head displacement was d, the perpendicular and parallel strain of the specimen surface can be described as:

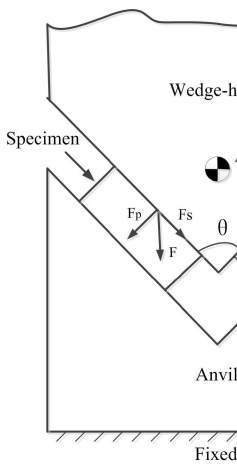

Figure 4. Schematic drawing of specimen showing forces.

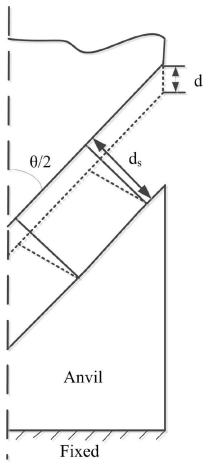

Figure 5. Deformation analysis of specimen.

$$\varepsilon_p = \frac{d\cos\frac{\theta}{2}}{d_s} \tag{2}$$

$$\varepsilon_s = \frac{d\sin\frac{\theta}{2}}{d_s} \tag{3}$$

Where d_s is the length of specimen, ε_p is the compressive strain and ε_s is the shear strain of specimen.

3.2 Pressure and Temperature Results: Analysis of No-React Specimen

Figure 6 shows the variation of pressure and temperature with time measured using a pressure sensor and a thermocouple below the specimens. There are two stress peaks and one temperature peak. As can be seen in Figure 6(c), the specimens did not react. Analysis of the high-speed photographs shows that after impact of the drop-weight with the wedge-head, the wedge-head velocity was greater than the drop-weight. For 700 μs, the first peak of stress was generated due to specimen compaction, then the stress decreased as the specimen crushed and jetted. At

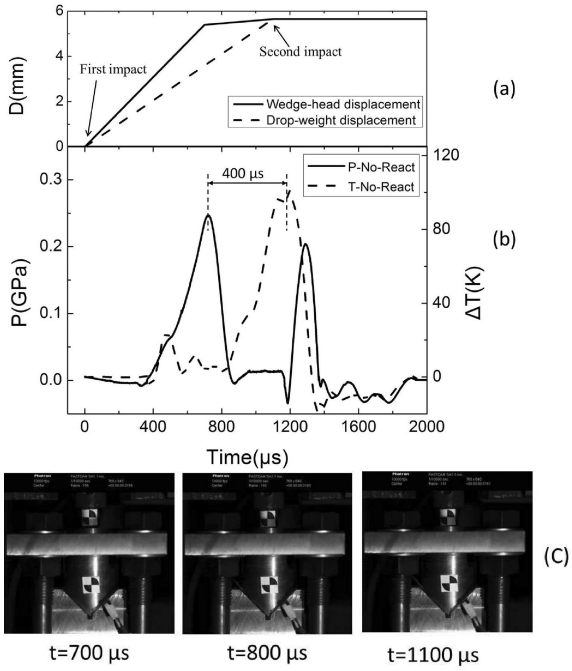

Figure 6. (a) Drop-weight and wedge-head displacement versus times, (b) Pressure and temperature versus times, (c) selected high-speed photographs.

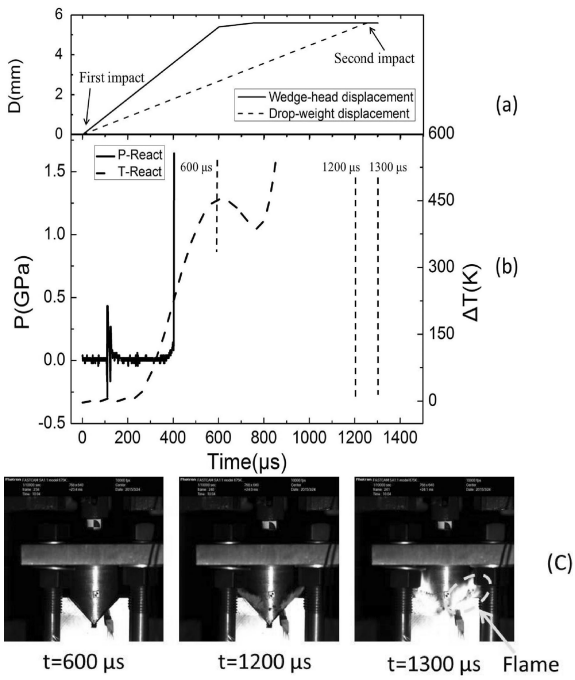

Figure 7. (a) Drop-weight and wedge-head displacement versus times,(b) Pressure and temperature versus times, (c) selected high-speed photographs.

1100 μs, a second impact occurred due to the drop-weight catching up with the wedge-head. The stress of the first peak was significantly higher than the second peak. Throughout the process, no reaction was observed. The temperature curves show that the maximum temperature rise was 99 K, much less than the ignition temperature (460 K) of the explosive. Frictional heating along with plastic deformation contributes to the energy increase. However, if the energy increase is less than the conduct on losses, reaction is not supportted, so the temperature decreased. The first peak of the temperature curve is due to the accumulation of energy. It is not the same as stress accompanied with impact synchronization, so the first temperature peak occurred 400 μs later than the first stress peak (Figure 6(b)).

3.3 Pressure and Temperature Result: Analysis of React Specimen

Figure 7 shows the drop-weight and wedge-head displacement versus time, pressure and temperature curves of a PBX specimen which reacted. After the first impact of the drop-weight with the wedge-head, the velocity of the wedge-head was greater than the drop-weight. The first stress peak occurred at 100 μs, and decreased subsequently. However, the stress increased suddenly at 400 μs, due to the pressure sensor becoming damaged. At the same time, the stress curves increased rapidly. At 600 μs, due to friction and plastic deformation, the temperature reached 450 K, the specimens being completely crushed at this first time, and the temperature soon started to decrease. the wedge-head did not move between 750 μs to 1200 μs, then the second impact occured between the drop-weight and the wedge-head. When the specimens were compressed and sheared the second time, the temperature increased to 560 K. However, the thermocouple was destroyed by the second impact. High-speed photography was used to diagnose when the explosive reacted in this set of experiments. Images with a resolution of 768 × 640 pixels and a frame rate of 10000 fps were obtained. as can be seen in Figure 7. At 1200 μs there was no flame. However, there was strong light output at 1300 μs. So, it can be confirmed, the explosive reacted between of 1200 and 1300 μs.

In these PBX experiments, thermocouples and pressure sensors were easily destroyed so that they can not measure the data precisely. Further experiments were performed using an infrared camera to observe the temperature of explosive flames. In previous studies, heat sensitive film was used to observe whether shear bands or hot-spots developed [6]. In our experiments, the maximum flame temperature variation of the explosive was measured. In Figure 8, the jet powder temperature rose by 80 K due to complete crushing of the specimen by 600 μs. In the impact process, specimens were compressed and sheared between the wedge-head and wedge-surfaces. Then plastic deformation occurred, with the energy accumulating up to the threshold of ignition, so that the PBX explosive reacted. At 1300 μs,

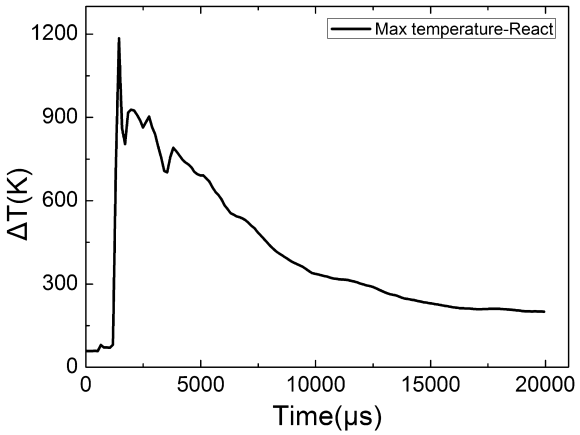

Figure 8. Temperature versus times.

the flame temperature had risen by 740 K accompanied by vigorous reaction of the PBX. At this stage, because heat loses were less than heat generation, the temperature continued to increase up to the maximum temperature of 1180 K. After 1400 μs, the loss of heat was greater than the heat generated, so that the temperature began to decrease towards room temperature.

3.4 Comparing React and No-React Results

Figure 9 illustrated whether the specimen reacted as the wedge-head velocity was varied and the time interval between the first and second impacts. With the aid of DIC analysis, it seems reasonable to conclude that both the wedge-head velocity and the time interval of impact contributes to the reaction of the specimen. However, there is no obvious pattern as to whether the specimen reacted within the dashed line.

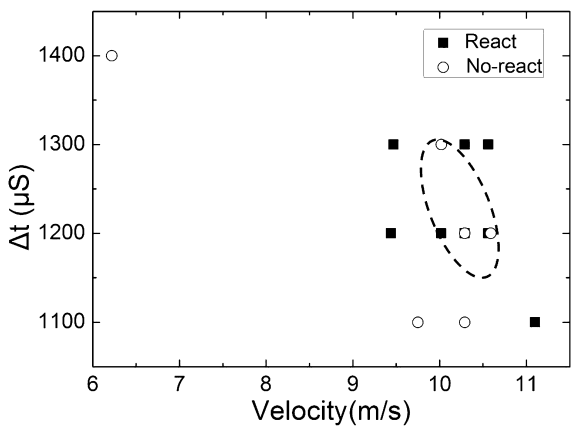

Figure 9. Result of specimen react/no-react with wedge-head impact velocity.

Figure 10 shows the variation of temperature of the PBX explosive measured using a thermocouple for the react and no-react cases. It is obvious that the temperature rise for the react case is higher than for the no-react. The maximum temperature rise of react was 550 K, which exceeds the reaction threshold temperature (460 K) of the PBX explosive. The thermocouple was destoryed later. As the loading continued, flame can be seen jetting from the wedge-surface in the high-speed photographs at 1300 μs (Figure 7 (c)). In contrast, the maximum temperature rise was 97 K for the no-react case, which did not reach the reaction threshold. The specimen was simply crushed and had a finite temperature rise at the second impact. The reason may be that the induced energy of the second impact was not enough to support self-sustianing reaction before the temperature decreased. However the PBX reaction can generate enough energy to support continous reaction so that the temperature can rise again.

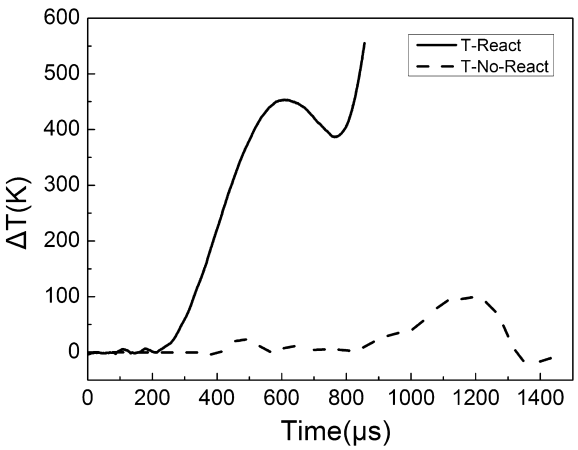

Figure 10. Temperature variation with time for the react and non-react cases.

3.5 Result of XRD Analyze

In order to quantitativly analyse the change of components under the same experimental conditions, X-ray diffraction (XRD) was used to analyze the different material compositions. In this set of experiments, raw-material, recovered no-react and reacted specimens were investigated with the diffraction angle 2θ between 5° and 53° under the same condition (Figure 11). Only the RDX and Al peaks are considered in the measurements. In the diffractiongrams, the 2θ angle peaks of 38.4° and 44.7° correspond to Al, the other peaks were due to RDX. As shown in Figure 11, the RDX crystal structure of both the no-react and reacted material were changed compared with the raw material, this maybe the reason that induces the PBX sensitivity. The volume fraction of Al was determined by XRD comparison (Table 1). It can

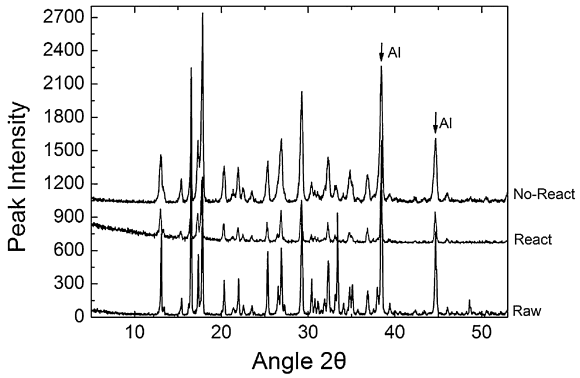

Figure 11. X-ray diffraction, 2θ-range between 5°and 53°(Raw material No-React material and React material).

Table 1. Volume fraction of Al in a raw specimen and recovery specimens of no-react and react.

	Volume fraction of Al (%)
Raw specimen	17.1
No-react specimen	20.9
React specimen	15.9

be concluded that the relative volume fraction of Al decreased after react.

4 Conclusion

This paper has been proposed a new method to research the compression and shear of a PBX under the drop-weight loading. The PBX under loading from impact to reaction undergoes crushing, melting and ignition. Compared with loading by a split Hopkinson pressure bar [18], drop-weight loading time is longer and the PBX reacts more easily under combined compression and shear loading. At the same time, the specimen temperature was measured using a thermocouple. Regarding the impact ignition threshold, there was a relation not only with the impact velocity of the wedge-head, but also with the loading time interval between first and second impacts.

XRD results clearly show that the RDX crystal structure changes under impact loading. The PBX was damaged by the first impact, and hence ignited more easily at the second impact. However, there would be no reaction if the pressure was not enough for ignition of the damaged specimen. Therefore, more studies are needed about the ignition detailed mechanisms for drop-weight to understand the ignition threshold.

References

[1] S. J. P. Palmer, J. E. Field, J. M. Huntley, Deformation, Strengths and Strains to Failure of Polymer Bonded Explosives, *Proc. R. Soc. London Ser. A* **1993**, 440, 399–419.
[2] P. Chen, H. Xie, F. Huang, T. Huang, Y. Ding, Deformation and Failure of Polymer Bonded Explosives Under Diametric Compression Test, *Polym. Test.* **2006**, 25, 333–341.
[3] Y. Wu, F. L. Huang, A Microscopic Model for Predicting Hot-spot Ignition of Granular Energetic Crystals in Response to Drop-weight Impacts, *Mech. Mater.* **2011**, *43*, 835–852.
[4] J. E. Balzer, J. E. Field, M. J. Gifford, W. G. Proud, S. M. Walley, High-speed Photographic Study of the Drop-Weight Impact Response of Ultrafine and Conventional PETN and RDX, *Combust. Flame* **2002**, *130*, 298–306.
[5] D. M. Williamson, S. J. P. Palmer, W. G. Proud, Fracture Studies of PBX Simulant Materials, *ShocK Compression of Condensed Matter.* **2005**, *845*, 829–832.
[6] J. E. Balzer, W. G. Proud, S. M. Walley, J. E. Field, High-speed Photographic Study of the Drop-weight Impact Response of RDX/DOS Mixture, *Combust. Flame* **2003**, *135*, 547–555.
[7] M. H. Keshavarz, H. R. Pouretedal, Simple Empirical Method for Prediction of Impact Sensitivity of Selected Class of Explosives, *J. Hazard. Mater.* **2005**, *124*, 27–33.
[8] A. C. Mcintosh, J. Brindley, J. F. Griffiths, An Approximate Model for the Ignition of Reactive Materials by a Hot Spot with Reactant Depletion, *Mathematical and Computer Modelling.* **2002**, *36*, 293–306.
[9] J. Brindley, J. E. Griffiths, A. C. Mclntosh, Ignition Phenomenology and Criterial Associated with Hotspots Embedded in a Reactive Material, *Chem. Eng. Sci.* **2001**, *56*, 2037–2046.
[10] R. W. Armstrong, H. L. Ammon, W. L. Elban, D. H. Tsai, Investigation of Hot Spot Characteristic in Energetic Crystals, *Thermochim. Acta* **2002**, *384*, 303–313.
[11] Y. Wu, F. L. Huang, A Microscopic Model for Predicting Combined Damage of Particles and Interface Debonding in PBX Explosives, *Mech. Mater.* **2009**, *41*, 27–47.
[12] E. S. Collins, B. R. Skelton, M. L. Pantoya, F. Irin, M. J. Green. Ignition Sensitivity and Electrical Conductivity of an Aluminum Fluropolymer Reactive Material with Carbon Nanofillers, *Combust. Flame* **2014**.
[13] M. N. Raftenberg, W. M. Jr, G. C. Kirby, Modeling the Impact Deformation of Rods of a Pressed PTFE/Al Composite Mixture, *International Journal of Impact Engineering.* **2008**, *35*, 1735–1744.
[14] H. Czerski, W. L. Perry, P. M. Dickson, Solid State Phase Change in HMX During Dropweight Impact, *13th Symposium (International) on Detonation,* Norfolk, VA, USA, July 23–28, **2006**.
[15] E. M. Hunt, S. Malcolm, M. L. Pantoya, F. Davis, Impact Ignition of Nano and Micron Composite Energetic Materials, *International Journal of Impact Engineering.* **2009**, *36*, 842–846.
[16] C. Gruau, D. Picart, R. Belmas, E. Bouton, E. Delmaire-sizes, J. Sabatier, H. Trumel, Ignition of a Confined High Explosive Under Low Velocity Impact, *International Journal of Impact Engineering.* **2009**, *36*, 537–550.
[17] V. S. Joshi, Recent Developments in Shear Ignition of Explosives Using Hybrid Drop Weight-Hopkinson Bar Apparatus, *Shock Compression of Condensed Matter.* **2007**, *955*, 945–950.
[18] J. G. Qin, Experimental Investigation and Numerical Modelling of Non-shock Ignition Mechanism in PBX Explosives, *National University of Defense Technology* Ph.D. Thesis, **2014**.

Received: March 14, 2018
Published online: November 15, 2018

